Synthesis of highly magnetic graphite-encapsulated FeCo nanoparticles using a hydrothermal process

2011 Nanotechnology 22 375603

(http://iopscience.iop.org/0957-4484/22/37/375603)

Nanotechnology **22** (2011) 375603 (7pp) doi:10.1088/0957-4484/22/37/375603

Synthesis of highly magnetic graphite-encapsulated FeCo nanoparticles using a hydrothermal process

Seung Jae Lee[1,2], Jee-Hyun Cho[3], Chulhyun Lee[3], Janggeun Cho[3], Yong-Rok Kim[2] and Joung Kyu Park[1]

[1] Center for Nano-Bio Fusion Research, Korea Research Institute of Chemical Technology, Daejeon, 305-600, Korea
[2] Department of Chemistry, Yonsei University, Seoul, 120-749, Korea
[3] Division of Magnetic Resonance Research, Korea Basic Science Institute, Ochang, 363-883, Korea

E-mail: parkjk@krict.re.kr

Received 10 May 2011, in final form 19 July 2011
Published 18 August 2011
Online at stacks.iop.org/Nano/22/375603

Abstract
The graphite encapsulation of metal alloy magnetic nanoparticles has attracted attention for biological applications because of the high magnetization of the encapsulated particles. However, most of the synthetic methods have limitations in terms of scalability and economics because of the demanding synthetic conditions and low yields. Here, we show that well controlled graphite-encapsulated FeCo core–shell nanoparticles can be synthesized by a hydrothermal method, simply by mixing Fe/Co with sucrose as a carbon source. Various Fe/Co metal ratios were used to determine the compositional dependence of the saturation magnetization and relaxivity coefficient. Transmission electron microscopy indicated that the particle sizes were 7 nm. In order to test the capability of graphite-encapsulated FeCo nanoparticles as magnetic resonance imaging (MRI) contrast agents, these nanoparticles were solubilized in water by the nonspecific physical adsorption of sodium dodecylbenzene sulfonate.

(Some figures in this article are in colour only in the electronic version)

1. Introduction

Magnetic nanoparticles with tailored surface modifications have been widely used experimentally for numerous *in vivo* applications such as magnetic resonance imaging (MRI) contrast enhancement, tissue repair, hyperthermia, medical diagnostics, therapeutics, and drug delivery [1–9]. These magnetic nanoparticles combine the beneficial magnetic properties of the core with possible functionalization of the surface. Recently, because of their high magnetization, metal alloy magnetic nanoparticles, such as FeCo, have been developed for MRI probes [10–12]. Thus far, degradation of nanocrystalline FeCo as a result of oxidation and the potential toxicity of Co have prevented the use of FeCo in biological applications [13]. In order obtain much higher magnetic moments of the metal alloy magnetic nanoparticles and more stability, the magnetic core could be protected by an additional surface coating that is chemically inert toward air and acids, and stable at elevated temperatures. The encapsulation of FeCo magnetic nanoparticles in carbon graphite is of particular interest since this could prevent their degradation in reactive chemical environments and isolate the particles magnetically from each other to avoid low-proximity interactions [10, 14, 15]. Graphite encapsulation has been achieved by the electrical arc-discharge technique [16–20], and pyrolysis of non-graphitizing carbon materials [21, 22]; however, these synthetic methods have limitations in terms of scalability and economics because of the demanding synthetic conditions and generally low yields. Here, we show that well controlled graphite-encapsulated FeCo core–shell (7 nm in size) nanoparticles can be synthesized by a hydrothermal method, simply by mixing Fe/Co with sucrose as a carbon

Table 1. Analysis of ICP-AES for different fractions of Fe/Co nanoparticles. (Samples 1, 2, 3, 4, and 5 with 0.3/0.7, 0.4/0.6, 0.5/0.5, 0.6/0.4, and 0.7/0.3, respectively.)

	Fe (wt%)	Co (wt%)	Total (wt%)	Fe ratio	Co ratio
Sample 1	29.9	55.6	85.5	0.35	0.65
Sample 2	37.2	49.3	86.5	0.43	0.57
Sample 3	42.5	44.2	86.7	0.49	0.51
Sample 4	48.6	36.7	85.3	0.57	0.43
Sample 5	56.8	28.0	84.8	0.67	0.33

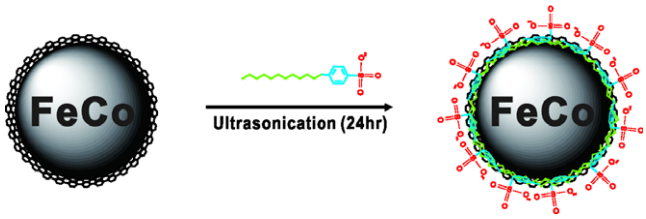

Scheme 1. Sodium dodecylbenzene sulfonate (NaDDBS) functionalized graphite-encapsulated FeCo nanoparticles.

source. The method reported here offers high production yields with reduced production costs and is environmentally friendly as a result of the simple equipment, readily available source materials, absence of explosive or corrosive gases, and only use of de-ionized water as the reaction medium. In addition, we describe the potential use of graphite-coated FeCo nanoparticles as MRI contrast agents in terms of various Fe/Co metal ratios.

2. Experimental details

2.1. Synthesis of the FeCo/C nanoparticles

In a typical experiment, graphite-encapsulated FeCo core–shell nanoparticles were formed by a simple hydrothermal reaction and a subsequent heat-treatment process at various temperatures (temperatures = 600, 800, 1000 and 1200 °C). In a typical reaction, a mixture, consisting of iron (III) nitrate enneahydrate ($Fe(NO_3)_3{\cdot}9H_2O$, 0.3–0.7 mmol, 99.0%, Kanto Chemical), cobalt (III) nitrate hexahydrate ($Co(NO_3)_2{\cdot}6H_2O$, 0.3–0.7 mmol, 99.0%, Kanto Chemical) and sucrose ($C_{12}H_{22}O_{11}$, 2.9 mmol, reagent grade, Aldrich) as a carbon source, was stirred vigorously to form a clear solution, and then placed in a 45 ml capacity stainless steel autoclave, which was heated in an oven to 190 °C for 9 h. The products were washed several times with distilled water, filtered off, and finally dried in a drying oven at 80 °C for 5 h. Subsequently, the dried products were heat-treated at 600, 800, 1000 and 1200 °C for 3 h under an Ar atmosphere to grow a carbon graphite shell on the surface of the FeCo nanoparticles. The hydrothermal treatment at a pressure of 15 bars induces dehydration of the carbohydrate and carbonization, resulting in carbon sources positioned predominantly near the cores of the FeCo nanoparticles. Consequently, a graphite shell grows on the FeCo core during annealing in an Ar atmosphere, resulting in graphite-encapsulated FeCo core–shells. Annealing of the FeCo/C core–shell structures at 1000 °C (optimum temperature) for 3 h leads to graphite shell growth and highly ordered crystallinity. It seems that the graphite shell minimizes crystal growth and aggregation during this high temperature annealing. We also confirmed the Fe/Co metal ratios in the FeCo/C nanoparticles using inductively coupled plasma atomic emission spectroscopy (ICP-AES) (table 1).

2.2. Synthesis of water soluble FeCo/C nanoparticles

Sodium dodecylbenzene sulfonate ($CH_3(CH_2)_{11}C_6H_4SO_3Na$, NaDDBS, Aldrich), which consists of a benzene ring moiety, a charged group, and an alkyl chain, significantly enhances the stability of carbon nanotubes in water [27]. Hence, the graphite-encapsulated nanoparticles were surface functionalized with NaDDBS surfactant to make them soluble in water (scheme 1). Briefly, the FeCo/C nanoparticles were mixed with NaDDBS surfactant (1:10 weight ratio) in 3 ml of distilled water. The mixture was sonicated for 24 h at 30 °C and the coated nanoparticles were separated magnetically and washed with water to remove the unreacted NaDDBS.

2.3. Characterization

The graphite-encapsulated nanoparticles were identified using a Rigaku D/MAX-2200V x-ray diffractometer (XRD) using Cu Kα radiation (λ = 1.5406 Å). Transmission electron microscopy (TEM) and high-resolution TEM (HRTEM) images were obtained using a JEM-2100F field emission electron microscope at an accelerating voltage of 200 kV. Samples for TEM were prepared by spreading drops of the solution samples on copper grids coated with a carbon film followed by drying in the oven at 60 °C. Raman spectroscopic measurement of the FeCo/C nanoparticles was carried out using a Senterra Dispersive Raman System (Brucker, Germany) with 632.8 nm. FT-IR spectra were obtained with a Thermo Nicolet 5700 ATR spectrometer with single- and multi-bounce ATR accessory. A universal ATR sampling accessory was used to record the attenuated total reflection spectra of FeCo/C, pure sodium dodecylbenzene sulfonate (NsDDBS) and NaDDBS functionalized FeCo/C nanoparticles. Thermogravimetric (TG) spectra of the samples were obtained with a TGA Q5000 analyzer under N_2 gas atmosphere (TA instrument). The stoichiometries of the Fe and Co ratios and the metal concentrations in the nanoparticles were determined by Thermo Scientific iCAP 6500 duo inductively coupled plasma atomic emission spectroscopy (ICP-AES). The magnetic properties were measured on a superconducting quantum interference device (SQUID) magnetometer (Quantum Design). Magnetic resonance imaging (MRI) was performed with a Bruker 4.7 T MRI instrument with a 72 nm volume coil at the Korea Basic Science Institute in Ochang. The T_2 values of various phantom solutions were obtained from the Carr–Purcell–Meiboom–Gill (CPMG) sequence at room temperature: TR = 10 s, 128 echoes with 7.4 ms even echo space, number of acquisitions = 1, spatial resolution = 391 μm × 391 μm, section thickness = 1 mm.

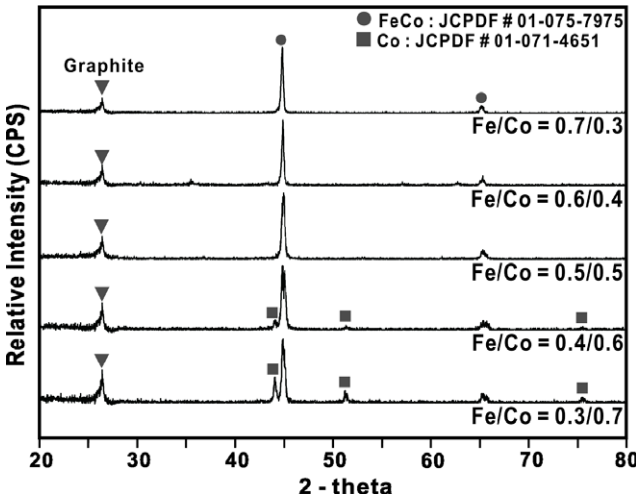

Figure 1. X-ray diffraction pattern of 7 nm nanoparticles in terms of Fe/Co fractions.

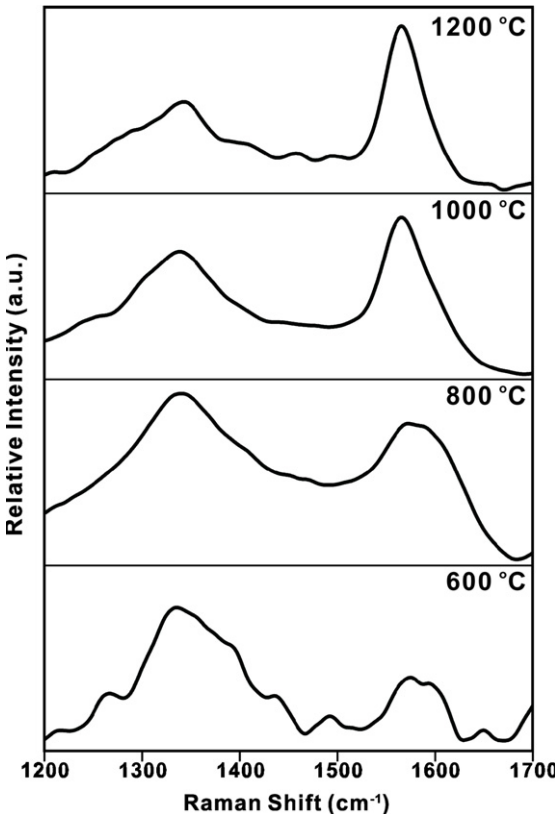

Figure 2. Raman spectra of FeCo/C nanoparticles in terms of annealing temperatures.

3. Results and discussion

The diffraction peak at about 26.2° can be assigned to the (002) planes of the hexagonal graphite structure, corresponding to the encapsulating graphite shells (figure 1); this indicates highly crystalline graphite. Further information about the graphite shell was obtained by Raman spectroscopy (figure 2). The two main peaks centered at 1340 cm^{-1} (D-band) and 1567 cm^{-1} (G-band) are in good agreement with the pattern reported for graphite in the literature [23, 24]. The intensity of the D-band decreased with annealing temperature. It can be said that the crystallinity of the graphite shell increased with increasing annealing temperature, since the origin of the D-band is associated with the disorder, lattice distortions, or amorphous carbon background signals [24, 25]. As can be seen from the XRD results (figure 1), in the case of Fe/Co = 0.3/0.7, a pure Co phase (JCPDF Card No. 01-071-4651) is detected but increasing concentrations of Fe reduced the amount of Co phase. Obviously, this result indicated that the concentration of Fe is the main factor for the formation of FeCo nanoparticles. A FeCo phase (JCPDF Card No. 01-075-7975) is detected for all samples and there are no detectable reflections in the XRD pattern from oxides, indicating that the core of the FeCo graphite nanoparticles is free from oxidation as a result of protection of the surface by the graphite shell. The XRD peak positions and relative intensities of these FeCo graphite shell nanoparticles show good agreement with a crystalline body-centered-cubic FeCo core. Figure 3 shows the normal TEM and HRTEM images of synthetic FeCo/C, revealing a spherical shape with an average core size of 7 nm. The crystalline body-centered-cubic FeCo core was identified by electron diffraction (inset in figure 3(b)).

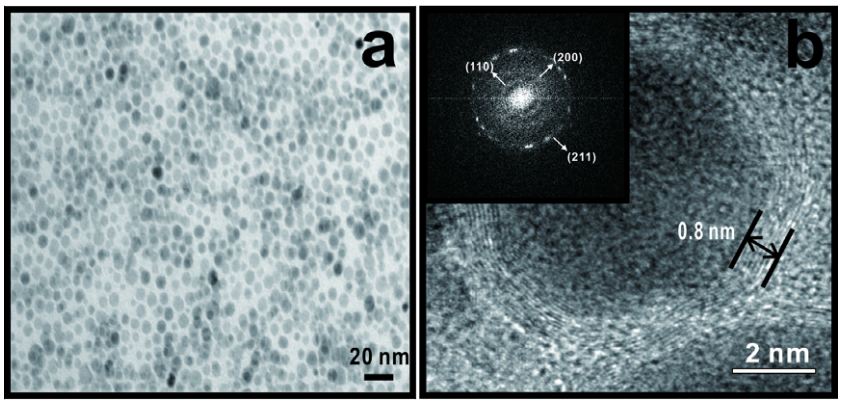

Figure 3. (a) TEM image of 7 nm Fe/Co = 0.6/0.4 nanoparticles. (b) High-resolution TEM image of Fe/Co = 0.6/0.4 nanoparticles. Inset: a selected-area electron diffraction pattern of Fe/Co = 0.6/0.4 nanoparticles.

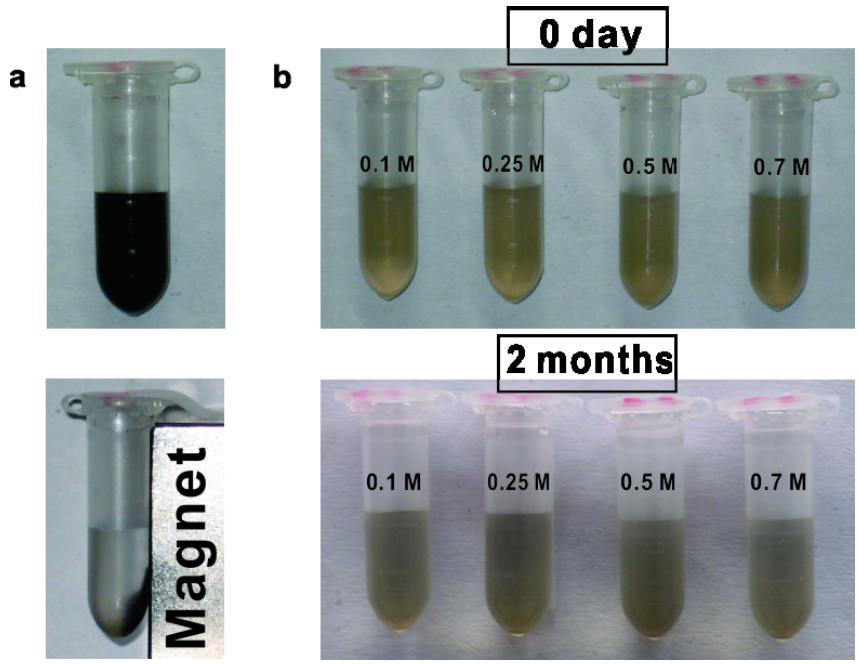

Figure 4. Colloidal stability of NaDDBS functionalized FeCo/C nanoparticles. (a) Photographs of water-dispersed NaDDBS functionalized FeCo/C nanoparticles (top) and magnetic separation of water-dispersed NaDDBS functionalized FeCo/C nanoparticles. (b) Colloidal stability against various NaCl solutions.

Strategies including chemical functionalization such as acid oxidation, and the use of anionic surfactants, have been successfully used for functionalization of the graphite surface. The chemical functionalization of carbon nanotubes is well known, and some effective methods have been identified, based the structural similarities between the graphite shells of magnetic nanoparticles and carbon nanotubes [26]. Sodium dodecylbenzene sulfonate (NaDDBS), which consists of a benzene ring moiety, a charged group, and an alkyl chain, significantly enhances the stability of carbon nanotubes in water [27]. Hence, the graphite-encapsulated nanoparticles were surface functionalized with NaDDBS surfactant to make them soluble in water (scheme 1). Briefly, the FeCo/C nanoparticles were mixed with NaDDBS surfactant (1:10 ratio) in 3 ml of distilled water. The mixture was sonicated for 24 h at 30 °C and the coated nanoparticles were separated magnetically and washed with water to remove the unreacted NaDDBS. The π-like stacking of the benzene rings onto the surface of the graphite and the surface coverage of the graphite by the NaDDBS made them soluble in water [28]. Figure 4 shows excellent colloidal and salt stability (NaCl) for the NaDDBS functionalized FeCo/C nanoparticles. The water soluble FeCo/C magnetic nanoparticles remain stable at room temperature for several days without noticeable precipitation and show good magnetic properties for a permanent Nd magnet, as shown in figure 4(a). Figure 4(b) shows excellent salt stability (NaCl) for the NaDDBS functionalized FeCo/C nanoparticles (nanoparticles:NaDDBS = 1:10) without significant aggregation over a period of two months. By contrast, these samples showed a poor salt stability with different concentrations of NaCl for seven days, as shown in figure 5(a), when the nanoparticles:NaDDBS ratio was decreased to the range of 1:1 to 1:5 by weight. These results indicated that the optimum ratio for NaDDBS was 1:10. Figure 5(b) shows the salt stability of NaDDBS functionalized FeCo/C nanoparticles with different concentrations of nanoparticles in 0.7 M NaCl solution. As can be seen in this figure, three samples (concentrations of FeCo/C of 3, 6, and 9 mg) show good salt stability for seven days. However, the 12 mg FeCo/C sample shows precipitation at the bottom after seven days. Moreover, we investigated the stability for the NaDDBS functionalized FeCo/C nanoparticles with 1:10 weight ratio in cell culture medium, and the resulting suspensions remained well dispersed for seven days; neither sedimentation nor aggregation of nanoparticles was observed under cell culture medium (figure 5(c)). As can be seen in figure 6(a), the Fourier-transform infrared (FT-IR) peak positions at 2956, 2923, and 1601 cm^{-1} of the NaDDBS functionalized FeCo/C nanoparticles show good agreement with CH_3 asymmetrical stretching, CH_2 asymmetrical stretching, and C–C aromatic stretching bands in the benzene ring, respectively. The strong peaks at 1177, 1042, and 674 cm^{-1} indicate S=O asymmetrical stretching, S=O symmetrical stretching, and $–SO_3–$ bending bands, respectively, which is in good agreement with the FT-IR patterns reported in the literature. The formation of NaDDBS functionalized FeCo/C nanoparticles was further confirmed by thermogravimetric (TG) comparison with FeCo/C nanoparticles, as shown in figure 6(b). It can be seen that the TG curve of the FeCo/C nanoparticles shows a weight loss above 600 °C, which corresponds to oxidation of the carbon shells to gaseous carbon oxides [29]. In the case of the TG curve of the NaDDBS functionalized FeCo/C nanoparticles, the onset of significant weight loss at 369.4 °C

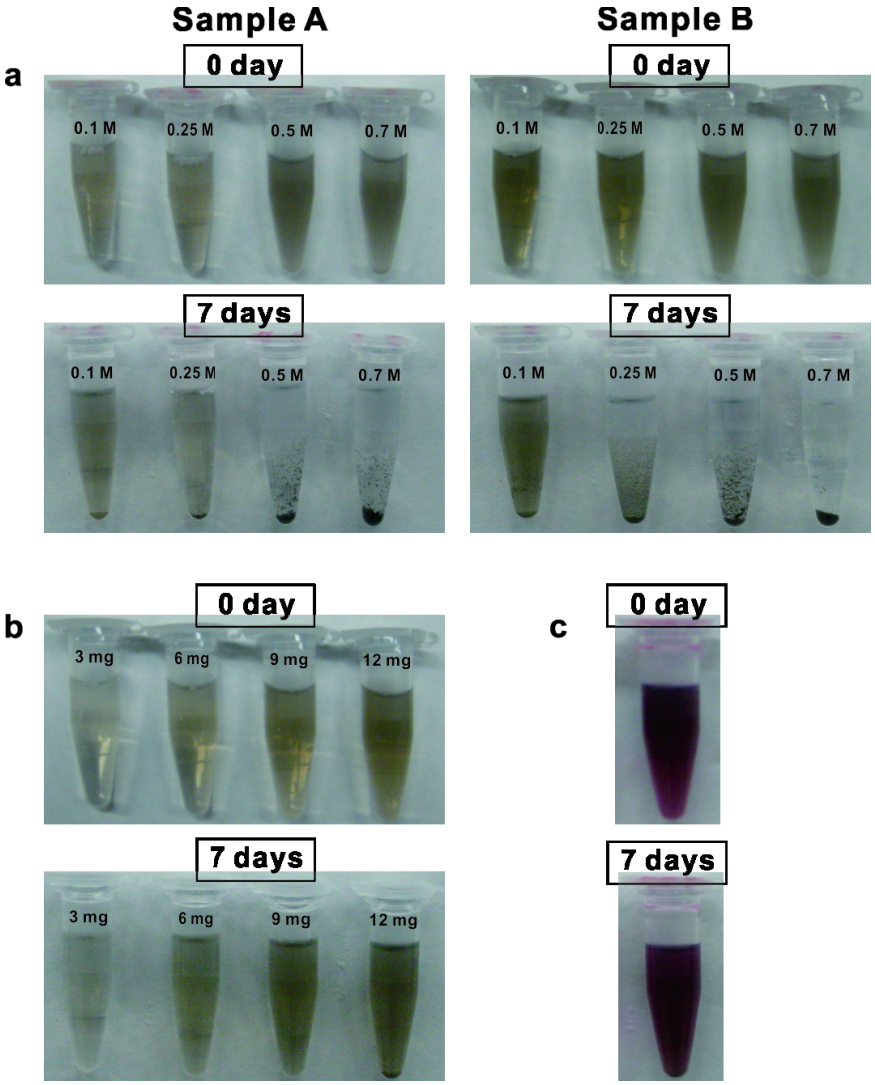

Figure 5. (a) Colloidal stability of NaDDBS functionalized FeCo/C nanoparticles with different NaDDBS ratios (Sample A nanoparticles:NaDDBS = 1:1, Sample B nanoparticles:NaDDBS = 1:5). (b) Colloidal stability of NaDDBS functionalized FeCo/C nanoparticles with different concentrations of FeCo/C. (c) Colloidal stability of NaDDBS functionalized FeCo/C nanoparticles in cell culture medium (condition of medium = DMEM, 5% FBS (fetal bovin serum), 1% P/S (penicillin/streptomycin)).

is much lower than that for FeCo/C nanoparticles; significant weight loss occurred in the range 369.4–502 °C, which is indicative of decomposition of the surface organics in this temperature range.

When we investigated FeCo/C nanoparticles with several different Fe/Co ratios using a SQUID magnetometer, the magnetization value (M_s, temperature = 300 K) increased with increasing Fe fraction (0.3–0.6 mole fraction) and then decreased at relatively high Fe contents (0.7 mole fraction), as shown in figure 7(a). In figure 7(a), the M_s values of FeCo/C nanoparticles with 0.3/0.7, 0.4/0.6, 0.5/0.5, 0.6/0.4, and 0.7/0.3 mole fraction were 129, 152, 226, 235, and 217 emu g^{-1}, respectively. The FeCo/C nanoparticles with a Fe/Co ratio of 0.6/0.4 showed the highest magnetization value of 235 emu g^{-1}. As these magnetization values were dependent on the composition of the Fe/Co mole fractions, we measured the transversal relaxation time (T_2)-weighted MR images for each sample at 4.7 T MRI system and obtained the relaxivity coefficient (r_2) for FeCo/C nanoparticles with various Fe/Co mole fractions. The relaxivities of FeCo/C nanoparticles with Fe/Co ratios of 0.3/0.7, 0.4/0.6, 0.5/0.5, 0.6/0.4, and 0.7/0.3 were 140, 252, 361, 392, and 324 mM^{-1} s^{-1}, respectively. The highest relaxivity coefficient (r_2), obtained as the gradient of the plot of the spin–spin relaxivity (R_2), was 392 mM^{-1} s^{-1} for nanoparticles with a Fe/Co ratio of 0.6/0.4, resulted in significant darkening of the MR images (figure 7(b)). T_2-weighted MR images showed darker and darker images for increased nanoparticle concentrations because the MR images were dependent on the concentration of nanoparticles. The FeCo/C nanoparticles with 0.6/0.4 ratio showed a darker image than the other samples at low concentration. The high relaxivity of FeCo/C nanoparticles with 0.6/0.4 ratio means that they could be used as high performance MRI contrast agents at lower doses than the other samples [30].

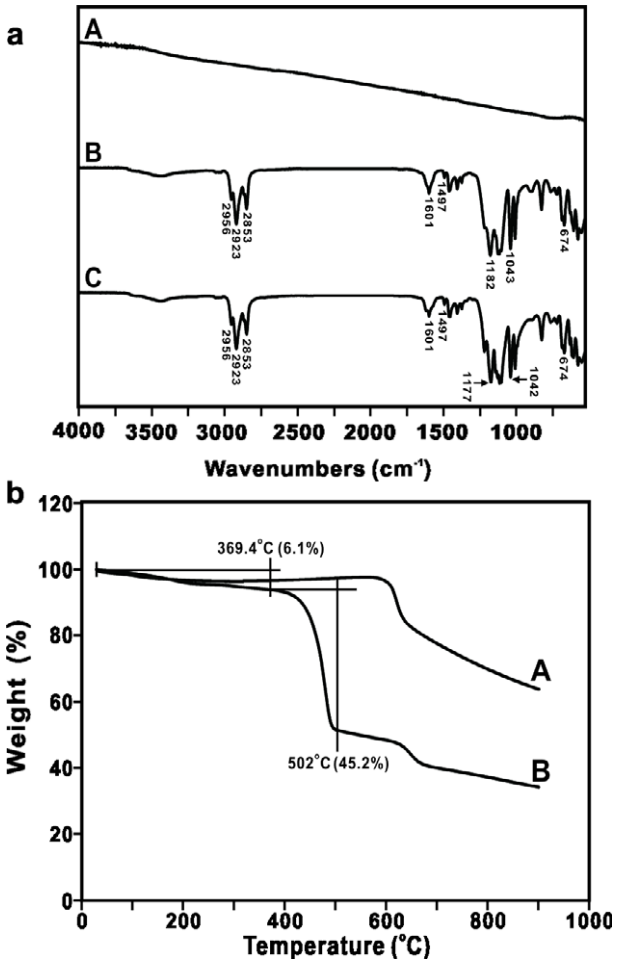

Figure 6. (a) FT-IR spectra of uncoated FeCo/C nanoparticles (A), pure NaDDBS (B), and NaDDBS functionalized graphite-encapsulated FeCo nanoparticles (C). (b) TG curves of uncoated FeCo/C nanoparticles (A) and NaDDBS functionalized carbon-graphite-encapsulated FeCo nanoparticles (B).

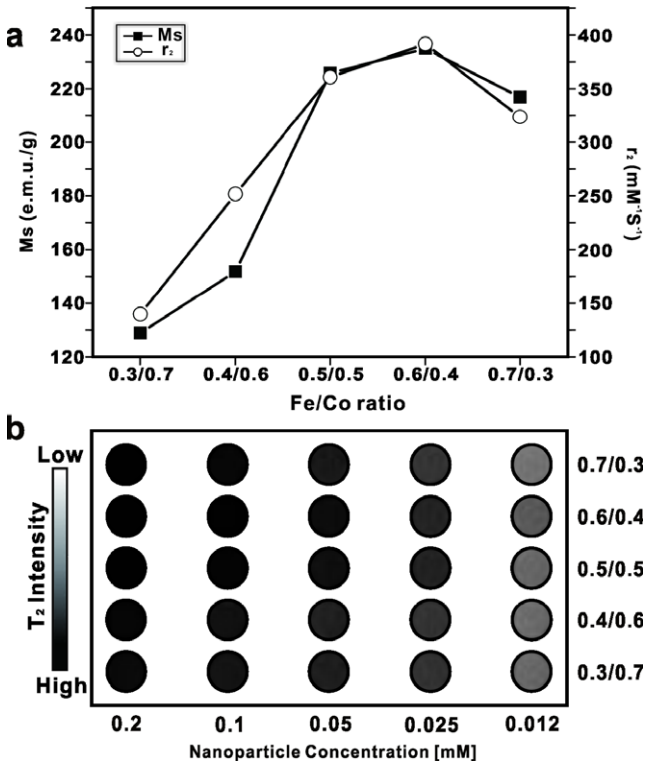

Figure 7. Fe/Co fraction dependent magnetization and MR contrast effect of FeCo/C nanoparticles. (a) Magnetization value (M_s, 300 K) and relaxivity coefficient value (r_2) of a series of FeCo/C nanoparticles. (b) T_2-weighted MR images in terms of metal concentrations.

4. Conclusion

Graphite-encapsulated FeCo core–shell nanoparticles with a particle size of 7 nm were synthesized by a hydrothermal method, simply by mixing Fe/Co and sucrose as a carbon source. The magnetization values and relaxivity coefficients of the nanoparticles are dependent on the Fe/Co ratio. FeCo/C nanoparticles with a Fe/Co ratio of 0.6/0.4 show the largest magnetization value (230 emu g^{-1}) and relaxivity coefficient (392 mM^{-1} s^{-1}). The FeCo/C nanoparticles, functionalized using sodium dodecylbenzene sulfonate, are fairly soluble and highly stable in water. The FeCo/C nanoparticles are attractive for various biological applications such as MR imaging and drug delivery because of their good magnetic properties and graphite shell.

Acknowledgments

This work was supported by Korea Research Council for Industrial Science and Technology (SI-1110). JKP acknowledges special support from SI-1104. Y-RK acknowledges support from a grant of the Korean Healthcare Technology R&D Project, Ministry for Health & Welfare Affairs (grant no. A085136). CHL thanks the Korea Basic Science Institute for grant no. T3122C.

References

[1] Weissleder R, Bogdanov A, Neuwelt E A and Papisov M 1995 *Adv. Drug Deliv. Rev.* **16** 321–34
[2] Lavan D A, Lynn D M and Langer R 2002 *Nature Rev. Drug Discov.* **1** 77–84
[3] Josephson L, Tung C H, Moore A and Weissleder R 1999 *Bioconjug. Chem.* **10** 186–91
[4] Bulte J W M *et al* 2001 *Nature Biotechnol.* **19** 1141–7
[5] Niemeyer C M 2001 *Angew. Chem. Int. Edn* **40** 4128–58
[6] Chouly C, Pouliquen D, Lucet L, Jeune J J and Jallet P 1996 *J. Microencapsul.* **13** 245–55
[7] Kats E and Willner I 2004 *Angew. Chem. Int. Edn* **43** 6042–108
[8] Huber D L 2005 *Small* **1** 482–501
[9] Lu A H, Salabas E L and Schuth F 2007 *Angew. Chem. Int. Edn* **46** 1222–44
[10] Seo W S *et al* 2006 *Nature Mater.* **5** 971–6
[11] Xu Y H, Bai J and Wang J P 2007 *J. Magn. Magn. Mater.* **311** 131–4
[12] Sherlock S P, Tabakman S M, Xie L and Hongjie D 2011 *ACS Nano* **5** 1505–12
[13] Reiss G and Hutteb A 2005 *Nature Mater.* **4** 725–6
[14] Turgut Z, Scott J H, Huang M Q, Majetich S A and McHenry M E 1998 *J. Appl. Phys.* **83** 6468–70
[15] Desvaux C, Amines C, Fejes P, Renaud P, Respaud M, Lecante P, Snoeck E and Chaudret B 2005 *Nature Mater.* **4** 750–3

[16] Ruoff R S, Lorents D C, Chan B, Malhotra R and Subramoney S 1993 *Science* **259** 346–8
[17] Dravid V P, Host J J, Teng M H, Elliott B, Hwang J, Johnson D L, Mason T O and Weertman J R 1995 *Nature* **374** 602
[18] Hayashi T, Hirono S, Tomita M and Umemura S 1996 *Nature* **381** 772–4
[19] Scott J H J and Majetich S A 1995 *Phys. Rev.* B **52** 12564–71
[20] Bokhonov B B 2011 *Carbon* **49** 2444–9
[21] Harris P J F and Tsang S C 1998 *Chem. Phys. Lett.* **293** 53–8
[22] Fernandez-Garcia M P, Gorria P, Sevilla M, Proenca M P, Boada R, Chaboy J, Fuertes A B and Blanco J A 2011 *J. Phys. Chem.* C **115** 5294–300
[23] Nemanich V L and Solin S A 1979 *Phys. Rev.* B **20** 392–401
[24] Tuinstra F and Koenig J L 1970 *J. Chem. Phys.* **53** 1126–30
[25] Boskovie B O, Stolojan V, Khan R U A, Haq S and Silva S R P 2002 *Nature Mater.* **1** 165–8
[26] Krause B, Petzol G, Pegel S and Potschke P 2009 *Carbon* **47** 602–12
[27] Islam M F, Rojas E, Bergey D M, Johnson A T and Yodh A G 2003 *Nano Lett.* **3** 269–73
[28] Liu J and Ducker W A 2000 *Langmuir* **16** 3467–73
[29] Jia X, Chen S, Jiao X, He T, Wang H and Jiang W 2008 *J. Phys. Chem.* C **112** 911–7
[30] Park J K, Jung J, Subramaniam P, Shah B P, Kim C, Lee J K, Cho J-H, Lee C and Lee K-B 2011 *Small* **7** 1647–52